Atmos. Chem. Phys. Discuss., 14, 23075–23123, 2014
www.atmos-chem-phys-discuss.net/14/23075/2014/
doi:10.5194/acpd-14-23075-2014

Atmospheric Chemistry and Physics Discussions

Analysis of the atmospheric composition during the summer 2013 over the Mediterranean area using the CHARMEX measurements and the CHIMERE model

L. Menut[1], S. Mailler[1], G. Siour[2], B. Bessagnet[3], S. Turquety[1], G. Rea[1], R. Briant[1], M. Mallet[4], J. Sciare[5], and P. Formenti[2]

[1]LMD, Laboratoire de Météorologie Dynamique, UMR CNRS 8539, Ecole Polytechnique, Ecole Normale Supérieure, Université P. M. Curie, Ecole Nationale des Ponts et Chaussées, Palaiseau, France
[2]LISA, Laboratoire Inter-Universitaire des Systèmes Atmosphériques, UMR CNRS 7583, Université Paris Est Créteil et Université Paris Diderot, Institut Pierre Simon Laplace, Créteil, France
[3]INERIS, Institut National de l'Environnement Industriel et des Risques, Verneuil en Halatte, 60550, Parc Technologique ALATA, France
[4]Laboratoire d'Aérologie, UMR CNRS 5560, Université P. Sabatier, Toulouse, France
[5]LSCE, Laboratoire des Sciences du Climat et de l'Environnement, UMR CNRS 8212, CEA, Université Versailles St Quentin, Gif sur Yvette, France

Received: 18 July 2014 – Accepted: 27 August 2014 – Published: 8 September 2014

Correspondence to: L. Menut (menut@lmd.polytechnique.fr)

Published by Copernicus Publications on behalf of the European Geosciences Union.

ACPD
14, 23075–23123, 2014

Abstract

The ADRIMED campaign provides measurements of all key parameters regarding atmospheric composition in the Mediterranean area during the summer 2013. This is an opportunity to quantify the ability of current models to adequately represent the atmospheric composition in this complex region, which is influenced by anthropogenic emissions from Europe, Africa, the Middle-East and from shipping activities as well as mineral dust emissions mostly from the arid areas in Africa, sea-salt emissions, biomass burning emissions and biogenic emissions from the vegetation. The CHIMERE model in its present version is a chemistry-transport model which takes into account all these processes. We show here by simulating the period from 5 June to 15 July 2013 with the CHIMERE model and comparing the results to both routine and specific ADRIMED measurements that this model allows an adequate representation the atmospheric composition over the western Mediterranean, in terms of ozone concentration, particulate matter (PM) and aerosol optical depth (AOD). It is also shown that the concentrations of PM on all the considered area is dominated by mineral dust, even though local dust emissions in Europe are certainly overestimated by the model. A comparison with sulphate concentrations at Cape Corsica exhibits some discrepancies related to the regridding of shipping emissions.

1 Introduction

Particulate matter is a major problem for regional air quality in Europe (EEA, 2013). During the last decade, the European legislation focused on particulate matter (PM) with PM_{10} (particles with a particle diameter below 10 µm) and even $PM_{2.5}$ in the last European directive on air quality (air quality directive 2008/50/EC). PM is responsible for a loss of life expectancy particularly when we consider long-term exposure to $PM_{2.5}$ (Kloog et al., 2012; Martinelli et al., 2013).

ACPD
14, 23075–23123, 2014

However, studying the sources and sinks of aerosols is very difficult since a lot of different components are included in these particulate matters: several chemical species or materials (organic matter, sulphates, nitrates, ammonium, mineral dust, sea salt, etc ...), with several sizes and shapes, several origins, lifetimes, potential direct and indirect effects on radiation, clouds formations etc. (Rodriguez et al., 2007). In order to reduce potential damages due to too high aerosols concentrations, it is thus necessary to improve our knowledge on all of these aspects.

Among many polluted regions in the world, Monks et al. (2009) highlight the Mediterranean area as a hot spot for its high variability of aerosol compositions and origin. Two main circulations are identified over the Mediterranean area: a North to South flow in the lowest layers and a South to North flow in the middle and upper tropospheric layers (Millan et al., 2005).

Kubilay et al. (2003) presented the several characteristics of the South to North African flow depending on the season: during the summer and autumn, the dust outbreaks are limited to upper troposphere and originated of Middle-East and North-Africa. The major dust outbreaks coming from central Sahara are observed during spring, with identification of particles in the whole tropospheric column. In addition, two other semi-permanent systems are present: the Azores anticyclone at the Western edge of the Mediterranean and a low pressure system in the East. This leads to frontal systems coming from the Atlantic Ocean and crossing the sea from West to East, as presented by Scheeren et al. (2003). A simple synthesis of these results is summarised in Fig. 1.

The strong Northern component of the flow pattern is due to a differential heating between North Africa (bare soil), the Mediterranean sea (with a daily sea surface temperature cycle) and the land of Southern Europe (with a mixed-type vegetation) (Millan et al., 1997). This circulation dominates in the boundary layer (typically the first two kilometres above ground). Kallos et al. (1998) showed that this transport of pollutants occurs during all seasons, but mainly during summer (due to a lack in wet removal). This is also shown by Israelevich et al. (2012). Pollutants are found in the entire troposphere with time scales for transport of four to six days. They affect air quality in

ACPD
14, 23075–23123, 2014

North Africa and the Middle East part of the Mediterranean region. Due to a lack of wet removal during these periods, the only efficient mechanism becomes the dry removal, much more slower than the wet one.

An important part of aerosol mass in the Mediterranean area comes from the African mineral dust. They may be transported through the Atlantic Ocean towards United States and Europe (Kallos et al., 2006). For the particular case of Europe, the particles are mainly transported in the free troposphere and mainly composed of mineral dust and, to a lesser extent, carbon due to fires. These particles may have two different impacts: (i) a direct impact through their sedimentation into the surface layer: they thus contribute to the PM concentration in the boundary layer, (ii) an indirect impact through their effects on meteorology (dynamics and microphysics) and photochemistry.

The need for a better understanding of the aerosols life cycle led to several dedicated fields campaigns such as MINOS in Crete (Lelieveld et al., 2002), ESCOMPTE over Marseille in France (Mallet et al., 2006), EUCARII campaign (Kulmala et al., 2011) as well as a lot of studies using surface measurements of aerosols concentrations (Querol et al., 2009), airborne measurements (Dulac and Chazette, 2003), optical thicknesses deduced from sunphotometers (Kubilay et al., 2003) or satellite data (Barnaba and Gobbi, 2004). More recently, remote-sensing surface measurements were dedicated to the quantification of dust optical properties and direct radiative forcing as in Bergamo et al. (2008); Basart et al. (2009); Mallet et al. (2013).

These measurements have been accompanied by significant regional model developments. Depending on the studied aerosol type, modelling studies have helped to better quantify the sources, transport and radiative impact of mineral dust, (Pérez et al., 2011; Nabat et al., 2012; Menut et al., 2013b; de la Paz et al., 2013), sea salt, (Jiménez-Guerrero et al., 2011) and vegetation fires (Turquety et al., 2014), among others.

The major part of these studies was devoted to the analysis of past events. Another possible use of these modelling systems is for short-term forecast. Over Europe, numerous regional systems were designed these last years (Menut and Bessagnet, 2010). In general, they calculate separately aerosol types, such as anthropogenic and

ACPD
14, 23075–23123, 2014

mineral dust. However, an accurate forecast needs to take into account all aerosol types in the same model to be fully representative of the regional atmospheric composition. In the present study we use such a complete system with the WRF and CHIMERE models. Integrating recent developments described in Menut et al. (2013a), the CHIMERE chemistry-transport model takes into account anthropogenic, biogenic, sea-salt, mineral dust and vegetation fires emissions. All these species constitute a complex mixture remotely transported and deposited.

During the summer 2013, the ADRIMED field campaign was organised to better understand the aerosol properties over the Mediterranean basin (Mallet, 2014). ADRIMED, that deals with the aerosols, radiations and climate interaction, is a part of the international CHARMEX (CHemistry-AeRosol Mediterranean EXperiment) program (Dulac et al., 2013). In order to launch intensive observations periods (especially aircraft operations) with the best probability of interesting events, many models were used to forecast the meteorology and chemical concentrations, including the WRF-CHIMERE system.

The purpose of this paper is to fully evaluate the simulations undertaken during the campaign using a wide set of surface, in situ and remote sensing observations. Section 2 presents the experimental framework of the ADRIMED campaign and the whole set of data (surface, soundings, aircraft measurements, satellite) used in this study. Section 3 presents the modelling system and the settings. Sections. 4, 5 and 6 present gaseous, aerosols optical depth and aerosols concentrations results for the studied period, respectively. Conclusions and perspectives are presented in Sect. 7.

2 The Mediterranean area and the ADRIMED project

This study is undertaken in the framework of the "Aerosol Direct Radiative Impact on the regional climate in the MEDiterranean region" (ADRIMED) project. ADRIMED is part of the international ChArMEx program (Dulac et al., 2013). CHARMEX aims at

ACPD
14, 23075–23123, 2014

assessing the present and future state of atmospheric chemistry in the Mediterranean area, and its impact on the regional climate, air quality, and marine ecosystems.

The main goal of ADRIMED is to assess the impacts of the direct and semi-direct radiative effect of aerosols on the regional climate of the Mediterranean. The project strategy is based on an integrated approach combining an intensive experimental field campaign and regional modelling of meteorology and chemistry-transport.

The experimental part of the project was done during the summer 2013 (June and July). All measurements showed that summer was not a highly polluted period. The observed gaseous and particles concentrations were moderate and often a complex mixture of many different sources: anthropogenic activities, biogenic emissions from vegetations, mineral dust transport and vegetation fires.

Figure 2 presents the location of vegetation fires detected during the whole summer 2013. The calculation was performed using the high-resolution vegetation model used in this study and presented in Turquety et al. (2014). The week number of first fire detection ranges from 1 (the first week of June 2013) to 12 (the last week of September 2013). It shows a majority of first fire event during the weeks 8 to 12, i.e. during September. These fires are mainly located in Portugal and Russia, and in a lesser extent, in Greece. For each model grid cell, the number of fire events is presented i.e. the number of different fires for each area (the data are projected on the model mesh presented hereafter). For a large majority of diagnosed fires, this number is one, showing there were not a lot of fires during this summer.

2.1 The routine surface measurements

Over the Mediterranean area, the routine measurements are mainly performed for chemical concentrations and not meteorological variables. In fact, there is no organised network able to distribute mesonet stations data with variables such as 2 m temperature, relative humidity and 10 m wind speed. These variables are measured country by country and not always reachable. In this study, the comparisons between measured

ACPD
14, 23075–23123, 2014

and modelled meteorological variables will be limited to the measurements performed directly during and for the ADRIMED experiment.

For regulatory pollutants (such as PM_{10}, $PM_{2.5}$, O_3), many measurements are routinely performed and well organised in homogeneous databases. For instance the EEA (European Environmental Agency) is responsible for the AirBase database, it contains air quality monitoring data and information submitted by the participating countries throughout Europe (http://www.eea.europa.eu/). Concentrations are hourly recorded and this study will focus on ozone and PM_{10} surface concentrations. Due to the coarse model resolution (50 km × 50 km), the comparison of NO_2 is irrelevant, and has therefore not been performed. In order to calculate scores and study time series, we retained specific sites with a first set of 8 "coastal background" stations and a second set of 9 "continental background" stations. Their location is displayed in Fig. 3 and details about their localization is explained in Table 1. They were chosen to be representative of various locations around the Mediterranean Sea: Spain, France and Italy, including Baleares, Corsica and Lampedusa islands. From all available routine stations, the selected stations are all "background" stations. This choice is mandatory if we want to compare surface concentrations to regional model, knowing that the simulations presented here have a 50 km × 50 km horizontal resolution.

2.2 The specific ADRIMED measurements

The experimental part included in-situ surface at two super (Lampedusa and Cape Corsica) and secondary (Minorca, Granada) sites, aircrafts (ATR-42 and Falcon-20 aircrafts) and spaceborne observations, as presented in Mallet (2014).

2.2.1 Surface measurements

For surface measurements, the super-sites of Lampedusa and Cape Corsica were equipped to monitor the main aerosol properties as the complete particle size distribution (fine and coarse fraction), the chemical composition, possible mixing, total mass

ACPD
14, 23075–23123, 2014

concentration, scattering and absorption, particle vertical profiles as well as downward shortwave (SW) and longwave (LW) fluxes. In addition, a quite similar in-situ instrumentation has been deployed onboard the ATR-42 for estimating microphysical, chemical and optical properties within aerosol plumes located in altitude and not detectable at the surface stations. In parallel, remote-sensing observations (passive and active) have been performed onboard the Falcon-20 during the 17 June to 5 July period to derive aerosol loading and microphysical properties for the whole atmospheric column as well as aerosol vertical profiles.

2.3 Airborne measurements

The ATR-42 aircraft was operated by the SAFIRE CNRS, CNES and Météo-France joint laboratory. Nine flights were done during the studied period. The flight numbers, date and decimal hour, corresponding Julian day of flight are reported in Table 2. Trajectories are very different from one flight to another and are represented in Fig. 4.

2.4 The satellite measurements

Numerous satellite observations are available, but only the MODIS (Moderate Resolution Imaging Spectroradiometer) data will be compared in this study to model outputs. Other satellite data will be more precisely analysed in companion papers, always for the ADRIMED campaign analysis.

The MODIS satellite products have been used for many years to study the amount and origin of aerosols in the Mediterranean area troposphere. Barnaba and Gobbi (2004) used these data to split relative contributions of aerosols on AOD (Aerosol Optical Depth). They showed that for the same particle size, its origin (maritime, continental or desert dust) may induce an AOD variability of one order of magnitude. During the studied year of 2001, the total amount of aerosol emissions was found to be the largest for dust (119 kTons day^{-1} with lowest values during winter), followed by maritime

ACPD
14, 23075–23123, 2014

aerosols (111 kTons day^{-1} more or less constant during the year) and finally continental aerosols (33 kTons day^{-1} with largest value during summer).

More recently, Levy et al. (2010) evaluated the MODIS AOD product over land, by comparison to AERONET sunphotometer data. They showed that there is a high correlation (R = 0.9) between the two AOD products, with a mean bias of ±0.05. In this study, we combine the two MODIS sensors, AQUA and TERRA, to build an unified AOD product, including the Deep Blue algorithm result (Hsu et al., 2004). Even if some biases are observed over long periods, Levy et al. (2010) showed this can be a problem only for long-term trends studies. For this study, it is reasonable to consider that MODIS data are completely relevant for comparisons to model outputs during the ADRIMED period. The AOD estimated at 550 nm is used in this study. Some sensitivity studies (Kaufman et al., 1997; Tanré et al., 1997) estimated the expected error of MODIS retrievals as ±(0.03 + 0.05 × AOD) over ocean and ±(0.05 + 0.2 × AOD) over land.

3 The modelling system

The modelling system is composed of several models: the WRF regional meteorological model, the CHIMERE chemistry-transport model and additional individual models for emissions fluxes estimations. All these models are integrated in a modelling platform usable both in analysis and forecast mode. For the vegetation fires emissions, satellite data are analysed to be used by the high resolution fire model (Turquety et al., 2014). The biogenic and mineral dust emissions fluxes depend on the meteorology, when the anthropogenic emissions are only dependent on the week day. The simulation was performed from the 1 June to the 15 July 2013.

3.1 The meteorological model WRF

The meteorological parameters are modelled with the non-hydrostatic WRF regional model in its version 3.2.1 (Skamarock et al., 2007). The model is used with a constant

ACPD
14, 23075–23123, 2014

horizontal resolution of 50 km × 50 km and 32 vertical levels from the surface to 50 hPa, as displayed in Fig. 5. This resolution enables simulations over a very large domain, including all kind of sources (anthropogenic, biogenic, mineral dust and fires) as well as various long-range transport events often observed between Africa and Europe.

The Single Moment-5 class microphysics scheme is used allowing for mixed phase processes and super cooled water (Hong et al., 2004). The radiation scheme is RRTMG scheme with the MCICA method of random cloud overlap (Mlawer et al., 1997). The surface layer scheme is based on Monin–Obukhov with Carslon–Boland viscous sub-layer. The surface physics is calculated using the Noah Land Surface Model scheme with four soil temperature and moisture layers (Chen and Dudhia, 2001). The planetary boundary layer physics is processed using the Yonsei University scheme (Hong et al., 2006) and the cumulus parameterization uses the ensemble scheme of Grell and Devenyi (2002).

The global meteorological fields of NCEP/GFS are hourly read by WRF using nudging techniques and for the main atmospheric variables (pressure, temperature, humidity, wind). In order to preserve both large-scale circulations and small scale gradients and variability, the "spectral nudging" was chosen. This nudging was evaluated in regional models, as presented in Von Storch et al. (2000). In this study, the spectral nudging was selected to be applied for all wavelength greater than ≈ 2000 km (wavenumbers less than 3 in latitude and longitude, for wind, temperature and humidity and only above 850 hPa). This configuration allows the regional model to create its own structures within the boundary layer but to follow the large scale meteorological fields.

3.2 The chemistry-transport model CHIMERE

CHIMERE is a chemistry-transport model able to simulate concentrations fields of gaseous and aerosols species at a regional scale. The model is off-line and thus needs pre-calculated meteorological fields to run. In this study, we used the version fully described in Menut et al. (2013a). The simulations are performed over the same horizon-

ACPD
14, 23075–23123, 2014

tal domain as the one used for WRF. For the vertical grid, the 32 vertical levels are projected on the 20 levels of the CHIMERE mesh, defined from the surface to 300 hPa.

The gaseous species are calculated using the MELCHIOR 2 scheme and the aerosols using the scheme developed by Bessagnet et al. (2004). This module takes into account species such as sulphate, nitrate, ammonium, primary organic matter (POM) and elemental carbon (EC), secondary organic aerosols (SOA), sea salt, dust and water. These aerosols are represented using ten bins, from 40 nm to 40 µm, in diameter. The life cycle of these aerosols is completely represented with nucleation of sulphuric acid, coagulation, adsorption/desorption, wet and dry deposition and scavenging. This scavenging is both represented by coagulation with cloud droplets and precipitation. The formation of SOA is also taken into account.

The anthropogenic emissions are estimated using the same methodology as the one described in Menut et al. (2012) but with the HTAP (Hemispheric Transport of Air Pollution) annual totals as input data. These masses were prepared by the EDGAR Team, using inventories based on MICS-Asia, EPA-US/Canada and TNO databases (http://edgar.jrc.ec.europa.eu/htap_v2). Biogenic emissions are calculated using the MEGAN emissions scheme (Guenther et al., 2006) which provides fluxes of isoprene and monoterpenes. In addition to this version, several processes were improved and added in the framework of this study. First, the mineral dust emissions are now calculated using new soil and surface databases (Menut et al., 2013b) and with a spatial extension of potentially emitting areas in Europe as described in Briant et al. (2014). Second, chemical species emissions fluxes produced by vegetation fires are estimated using the new high resolution fire model presented in Turquety et al. (2014). And, finally, the photolysis rates are explicitly calculated using the FastJX radiation module (version 7.0b), (Wild et al., 2000; Bian and Prather, 2002). The modelled AOD is obtained by summing the optical depth produced by FastJX for the 600 nm wavelength over the whole atmospheric column.

ACPD
14, 23075–23123, 2014

4 Analysis of ozone concentrations

The first step of comparisons between measurements and model is devoted to the analysis of ozone. This gaseous species reflects the amount of photo-oxidant pollution, especially during summertime periods. Two kinds of data are used in this section: (i) the routine surface measurements of the AirBase background stations and (ii) the airborne measurements done for ADRIMED with the ATR aircraft. The AirBase measurements are regular in time, being hourly, and are able to quantify if the model is able to simulate both the background values and the peaks during high pollution events. But, being only at the surface, these measurements are not dedicated to provide an information on the model behaviour in the whole troposphere and thus to have an interpretation on the ozone long range transport. The ATR measurements are thus complementary to surface observations, providing vertical ozone profiles at a given time. But unlike surface observations, they are very specific and do not reflect the overall situation of the atmospheric pollution over the whole Mediterranean area. The simulation resolution being $\Delta x = \Delta y = 50\,\mathrm{km}$, comparisons are not done with NO_2 surface measurements for questions of representativeness.

4.1 Ozone surface concentrations time series

For ozone, scores are calculated for daily maximum and daily mean values. Results are presented in Table 3 (daily maximum) and Table 4 (daily mean). The corresponding time series are presented in Fig. 6 for the daily maximum values only (the time series for the hourly values and over a period of more than one month are not readable). Results are split as a function of the AirBase surface station type, coastal or continental.

The scores reported in Table 3 are representative of the ability of the model to catch extreme events. Depending on the location, the model simulates lower or higher maximum daily values, compared to the measurements. But for all stations, the differences between the two is never more than $20\,\mu g\,m^{-3}$. The correlations are also very dispersed, with values ranging from 0.09 to 0.71. One can expect to have better corre-

ACPD
14, 23075–23123, 2014

lations over the continent than over the sea due to the formation processes of ozone. This is not always the case, showing the sensitivity of the model to estimate daily peaks over this complex region.

The scores in Table 4 are complementary and present scores for daily mean values. In this case, the complete diurnal cycle of the ozone formation is taken into account. The scores are often better than for the daily peaks, with values up to 0.74. The less correlated results are obtained for the locations of Malaga, Bastia and Gap, as already diagnosed with the daily peaks. This denotes a general inability of the model to represent ozone formation and transport over these areas. For these three sites, the problem is related to the low model resolution: these three sites being in mountainous or island areas, the subgrid scale variability of ozone is difficult to model. The scores over these Mediterranean sites are generally lower than the usual predictions of CHIMERE used in a forecast mode over the whole Europe (Honoré et al., 2008).

Time series of measured and modelled ozone daily maximum are displayed in Fig. 6. For the coastal stations, Ajaccio, Bastia and Zorita, the measured values show flatter time series than the modelled ones, explaining some low correlations as for Ajaccio and Bastia. When the model overestimates the concentrations in Ajaccio, it underestimates the concentrations in Bastia, even if the locations are close and located in Corsica Island. From a model point of view, this consists in two close (but not neighboring) grid cells. These high differences may be explained by zooming on the Corsica as displayed in Fig. 7: ozone surface concentrations (in ppb) are shown for the 17 June 2013, 12:00 UTC. For this day, and more generally for the whole ADRIMED period, surface ozone concentrations are very variable and constituted of very dense and isolated plumes. This explains the large variability of scores when comparing point by point model and surface measurements, even if the horizontal resolution is coarse.

The scores are better for continental stations as Champforgeuil and Agen. The model is able to catch the day to day variability with highest values recorded for the 16–17 June and 6–10 July. This corresponds to well establish polluted periods, but the maximum values of 140 $\mu g\,m^{-3}$ are far from high polluted events situations.

ACPD
14, 23075–23123, 2014

4.2 Ozone, meteorological vertical profiles with the ATR flights

The ozone concentrations measured during the ATR flights are averaged from 1 Hz to a 5 mn time step. The number of averaged data is reported in Table 2. With the model, the concentration corresponding to the location of the measurement is interpolated in time (between the two modelled hourly outputs), vertically (between the two model vertical levels) and horizontally (using a bilinear interpolation). The comparison between the modelled and measured ozone concentrations is presented in Fig. 8. The corresponding altitude, temperature (in °C) and mean wind speed (in $m\,s^{-1}$) are also presented, using the same abscissa axis.

Each flight lasts between two and three hours. In the altitude panels, we can see that the plane made several iso-altitude measurements, mainly at 4000 m and 6000 m. For meteorological data, the temperature is always very well simulated by the WRF model. The differences between model and measurements are very weak, except, for example, for flights 30 and 31 where the temperature is slightly underestimated by the model and in altitude. The wind is variable and there are differences between the model and measurements, mostly in terms of variability. Trends in wind are well simulated. Ozone is always a little over-estimated by the model, especially in altitude. This is probably a direct effect of boundary conditions that may be too strong for this period. The boundary chemical fields are derived from a global climate model and the summer of 2013 was moderated in terms of pollution: the climatology may thus induce a positive bias in the model. These flights within the marine boundary layer are a very good opportunity to evaluate ozone concentrations over the maritime surfaces. These concentrations are usually very high in models due to a lack of deposition. For the parts of flights near the surface, the model is mostly closer to the measurement. There are two peaks simulated by the model during flights 29 and 33 that are not measured: these modelled high ozone values correspond to local ozone plumes as presented in Fig. 7. However, the ozone peak close to the surface for the flight 30 is perfectly captured.

ACPD
14, 23075–23123, 2014

5 Analysis of Aerosols Optical Depth

The Aerosols Optical Depth (AOD) reflects the extinction of radiations by aerosols along the whole atmospheric column. This quantity being well and often measured, the comparison between model and measurements is a widely used way to estimate the model ability to reproduce aerosols plumes at the right time and the right place. Thus, AOD enables to see if the model is able to reproduce massive emissions of mineral dust over arid areas and vegetation fires. This is also a way to see if the main long range transport structures are correctly reproduced. However, comparisons of AOD have limitations: (i) being vertically integrated, there is no information on the vertical structure of the aerosol plume, (ii) they are sensitive to a small part of the aerosol size distribution. In this study, the CHIMERE outputs AOD are calculated at 600 nm, due to the fastJ algorithm used in the model.

5.1 Comparisons between MODIS and CHIMERE

The measured AOD at 550 nm is extracted from the MODIS satellite data over the period from 6 June to 15 July 2013. These AOD are calculated at 550 nm. Observations are first averaged on the model grid, and comparisons are done for collocated data in space and time, as displayed in Fig. 9. The MODIS map includes the AOD retrieved over ocean and over land. In addition and when the data are available, the AOD estimated using the deep-blue algorithm is used (Sayer et al., 2013).

The most important AOD values are recorded over the Atlantic Ocean, in a flow from Western Africa towards North America. Over continental areas (Sahara and Sahel) and over the Atlantic Ocean, the modelled AOD is slightly overestimated but the location of the main sources and plumes is very well reproduced.

Other significant values are recorded in the South of the Arabian Peninsula and the Eastern Africa. Up to $\phi = 35^{\circ}$ N, the AOD is very low and lower than 0.2. Over the Mediterranean sea, no plume is detected: this means than on average and over this whole period, there was no massive or persistent aerosol plumes.

ACPD
14, 23075–23123, 2014

5.2 Comparisons between AERONET and CHIMERE

Comparisons between modelled and measured AOD are also done using the AERONET data (level 1.5). Time series are presented in Fig. 10. When the station of Banizoumbou is located close to the mineral dust sources, the stations of Capo Verde and Dakar are directly under the plume. This explains that over the whole period, AOD values are important, ranging between 0.4 and 2. The day to day variability is also important and these time series show the highest AOD values during the period from 5 to 15 June (before ADRIMED intensive observations periods). A second period with high values is between the 27 and 30 June. For these African stations, the modelled AOD is very close to the measurements. The model is able to retrieve the observed day to day variability, even if, on average, modelled values are greater than observed ones for stations far away from the main Saharan dust sources.

Time series are also presented for the stations of Lampedusa, Forth Crete and Izana. This set of stations is representative of islands (for Lampedusa and Izana), and remote locations (Forth Crete). The measured AOD values are very small, always lower than 0.5. This clearly shows that during the whole period, no intense aerosol plume was observed all around the Mediterranean sea. The comparison results are worse than for the African stations, and the model tends to overestimate the AOD. The differences between modelled and measured AOD are more or less constant for all stations, but more visible on time series with very low measured values.

This slight overestimation may be due to several factors that can not be diagnosed only with the AOD, this quantity being an integrated budget of many possible contributions. This may be an overestimation of surface mineral dust emissions, a shift in the aerosols size distribution, or an underestimation of modelled dry deposition velocities. But, accounting for all these potential problems, the AOD is satisfactorily modelled compared to the AERONET measurements (themselves having possible errors and biases).

ACPD
14, 23075–23123, 2014

The Table 5 corresponds to statistical scores calculated over 10 AERONET stations. The number of observations is very variable from one station to another: if the Izana stations have 516 measurements values, the Forth Crete has only 108. These differences are certainly due to the cloud screening algorithm applied on the raw sunphotometer data to ensure that provided AOD are only due to aerosols. The correlation is variable from one site to another with values ranging from 0.12 (Ilorin) to 0.76 (Izana) and 0.85 (Lampedusa). The RMSE is very large, of the order of magnitude of the AOD value, showing the high variability of both model and measurements. Finally, model performances are good, showing that the new parameterizations of mineral dust implemented in CHIMERE are completely able to retrieve hourly and daily variability of aerosols due mainly to the dust load.

6 Analysis of PM_{10} concentrations

For the understanding of aerosols life cycle, the analysis of PM_{10} surface concentrations is complementary to the analysis of AOD. In this case, the information is only close to the surface but the concentration is representative of the whole size distribution spectrum up to a mean mass median diameter of 10 µm.

6.1 Surface concentrations time series

Table 6 lists the comparisons results. In order to compare the measurements and the model data, values are daily averaged and in $\mu g\,m^{-3}$. The number of values compared is very variable and mostly between 700 and 1000, corresponding to hourly data over the whole period. Italian stations are different and measurements are only daily, leading to a lower number of observations. Depending on the station the correlation ranges from very low (−0.03 for Cartagena and Agen, for example) to moderate (0.68 in Hyeres, 0.65 in Vercelli). For a major part of the stations, the bias remains low and less than $5\,\mu g\,m^{-3}$.

ACPD
14, 23075–23123, 2014

The corresponding time series of measured and modelled surface PM_{10} concentrations are presented in Fig. 11. On average, the background concentrations are well modelled for all sites. But some discrepancies appear when some peaks are modelled but not measured. For example, at the stations of Zorita, Malaga and Agen, large PM_{10} concentrations are modelled but the measurements do not show any peak. These peaks are sporadic and can thus be due to overestimated mineral dust or fires emissions. The lower bias on the AOD suggests that the whole column is correct, but that the surface concentrations are too large. This can be, partially, the problem of all deterministic Eulerian models, often too diffusive vertically. Another possibility is to have too important local emissions. A way to better understand this overestimation is to analyze the aerosols composition, as presented in Sect. 6.2.

6.2 Modelled PM speciation

For each site, the modelled aerosols composition is presented as surface time series in Fig. 12. The concentrations are shown here for the whole aerosols size distribution, i.e. from 0.04 µm to 40 µm. This is thus logical to have surface concentrations higher than the ones presented for the PM_{10} time series. All presented species are described as CHIMERE model species families (such as SOA) or primarily emitted species (such as POM, EC and the rest of anthropogenic dust called PPM here). The complete explanations about these species are provided in Menut et al. (2013a). For all presented time series, the most important contribution comes from mineral dust, with, at least, 50 % of the total mass. This mineral dust part is also responsible of the large peaks observed on the PM_{10} concentrations. The second most important contribution corresponds to sea salts. This effect is particularly important for sites on islands or near the coast as Lampedusa and Cape Corsica. For "continental background" stations such as Champforgeuil and Agen, the concentrations are lower than for the other stations and the relative part of sea salt becomes negligible. However, surface concentrations of mineral dust remain important for these stations suggesting that modelled local emissions are too large. The last most important contribution is for sulphates with large

ACPD
14, 23075–23123, 2014

concentrations modelled in Lampedusa and Malaga, among others. Finally, the relative contributions of POM and EC are very low in the total, showing that this period was not influenced by large vegetation fires events.

In order to link the information of surface concentrations, aerosols composition and vertical structure, Fig. 13 presents vertical profiles for the same stations as in Fig. 12 and for the 21 June 2013 at 12:00 UTC. Over Lampedusa, the main part of the aerosols profile is due to the long range transport of mineral dust from Africa. This is also the case for the Cape Corsica site, in altitude, with the same important plume at 3000 to 4000 m a.g.l. (above ground level). In addition, a contribution of $\approx 50\,\%$ of sulphates is observed close to the surface, certainly due to shipping emissions since CHIMERE does not take marine biogenic sulphur emissions.

In Zorita, the contributions are mainly due to mineral dust, sulphates and sea salts. There is no plume in altitude and the concentrations are low with a maximum of $12\,\mu g\,m^{-3}$. This is the same behaviour in Malaga and Agen. Finally, the vertical profile in Champforgeuil shows an important peak around 2000 m a.g.l.: this is partly due to the mineral dust observed in Lampedusa and Cape Corsica, with, in addition, non negligible concentrations of nitrates. For all these profiles, the vertical concentrations seem realistic and the relative contributions of mineral dust correspond to the main part of the aerosol composition.

Measurements of Calcium and Sulphate performed at Cape Corsica provide some clues on the capability of CHIMERE to reproduce the concentrations of two major compound of PM (Fig. 14). Considering that most of the dust in this region comes from the Sahara, a factor of 15 is used to convert Calcium in Dust (Putaud et al., 2004). This factor is uncertain but is used only to study the temporal variability of dust concentrations. For mineral dust and for this specific site, the model has difficulties to retrieve the timing of peaks. Regarding sulphates, we clearly see an overestimate of the modelled concentrations. A closer look at the model results indicate a sulphate pattern due to SO_2 shipping emissions. However the timing of some peaks is well reproduced by the model. This comparison shows the difficulty of the dust module to give the right

ACPD
14, 23075–23123, 2014

dust concentrations at the surface. Even for better documented sources like shipping emissions, discrepancies related to the emission regridding of such lineic sources are certainly responsible for the overestimation of the model simulations in this area.

7 Conclusions

In the framework of the CHARMEX project, a simulation of the atmospheric composition was carried out at the regional scale with the WRF and CHIMERE models, for meteorology and chemistry-transport respectively.

The simulation period ranges from 1 June to 15 July of 2013 and covers the whole period of the ADRIMED project intensive observation periods. The simulation domain covers all of Europe and the Northern half of Africa which allows to take into account major sources of pollution: anthropogenic, biogenic as well as vegetation fires and mineral dust.

The key pollutants of air quality studies are compared between measurements and model. At the surface, ozone and PM_{10} were compared to surface measurements of the AirBase network and to ADRIMED specific measurements done at Lampedusa and Cape Corsica. Using all aerosols concentrations, the Aerosols Optical depth is diagnosed and compared to the AERONET stations measurements. In addition, comparisons are done between the ATR flights for ozone concentrations and some meteorological variables.

The error statistics showed that the model is able to reproduce surface ozone concentrations, both the average values and the variability, even if we note an overestimate of ozone concentrations. The comparison between modelled and measured ozone concentrations along the flight trajectories is very satisfactory and confirm the high ozone concentration close to the sea surface that commonly simulated in chemistry transport models, and the altitude ozone concentrations are also well captured.

Regarding the PM_{10} ground concentrations the model is able to reproduce correct average values with rather low correlations. These low correlations are attributed to

ACPD
14, 23075–23123, 2014

the flat time series or the difficulties to capture the dust peaks at the right time. When looking at the AOD, the model performances are better meaning that the dust module is able to emit the right load of particles at the right time in arid zones. In Europe, the dust emissions are certainly overestimated. A comparison with sulphate concentrations in Cape Corsica exhibits some discrepancies related to the emission regridding of shipping emissions.

Acknowledgements. This study was partly funded by the French Ministry in charge of Ecology. We thank the SAFIRE joint laboratory and the CHARMEX program for providing us all campaign measurements used in this study. We thank the EEA for maintaining and providing the AirBase database of pollutants surface concentrations over Europe. We thank the principal investigators and their staff for establishing and maintaining the AERONET sites used in this study: Didier Tanré for Banizoumbou, Capo Verde and Dakar; Bernadette Chatenet and Jean-Louis Rajot for Zinder and Cinzana; Daniela Meloni and Alcide Di Sarra for Lampedusa.

References

Barnaba, F. and Gobbi, G. P.: Aerosol seasonal variability over the Mediterranean region and relative impact of maritime, continental and Saharan dust particles over the basin from MODIS data in the year 2001, Atmos. Chem. Phys., 4, 2367–2391, doi:10.5194/acp-4-2367-2004, 2004. 23079, 23083

Basart, S., Pérez, C., Cuevas, E., Baldasano, J. M., and Gobbi, G. P.: Aerosol characterization in Northern Africa, Northeastern Atlantic, Mediterranean Basin and Middle East from direct-sun AERONET observations, Atmos. Chem. Phys., 9, 8265–8282, doi:10.5194/acp-9-8265-2009, 2009. 23079

Bergamo, A., Tafuro, A. M., Kinne, S., De Tomasi, F., and Perrone, M. R.: Monthly-averaged anthropogenic aerosol direct radiative forcing over the Mediterranean based on AERONET aerosol properties, Atmos. Chem. Phys., 8, 6995–7014, doi:10.5194/acp-8-6995-2008, 2008. 23079

Bessagnet, B., Hodzic, A., Vautard, R., Beekmann, M., Cheinet, S., Honoré, C., Liousse, C., and Rouil, L.: Aerosol modeling with CHIMERE: preliminary evaluation at the continental scale, Atmos. Environ., 38, 2803–2817, 2004. 23086

ACPD
14, 23075–23123, 2014

Bian, H. and Prather, M.: Fast-J2: accurate simulation of stratospheric photolysis in global chemical models, J. Atmos. Chem., 41, 281–296, 2002. 23086
Briant, R., Menut, L., Siour, G., and Prigent, C.: Homogeneized modeling of mineral dust emissions over Europe and Africa using the CHIMERE model, Geosci. Model Dev. Discuss., 7, 3441–3480, doi:10.5194/gmdd-7-3441-2014, 2014. 23086
Chen, F. and Dudhia, J.: Coupling an advanced land surface-hydrology model with the Penn State-NCAR MM5 modeling system. Part I: Model implementation and sensitivity, Mon. Weather Rev., 129, 569–585, 2001. 23085
de la Paz, D., Vedrenne, M., Borge, R., Lumbreras, J., de Andrés, J. M., Pérez, J., Rodriguez, E., Karanasiou, A., Moreno, T., Boldo, E., and Linares, C.: Modelling Saharan dust transport into the Mediterranean basin with CMAQ, Atmos. Environ., 70, 337–350, doi:10.1016/j.atmosenv.2013.01.013, 2013. 23079
Dulac, F. and Chazette, P.: Airborne study of a multi-layer aerosol structure in the eastern Mediterranean observed with the airborne polarized lidar ALEX during a STAAARTE campaign (7 June 1997), Atmos. Chem. Phys., 3, 1817–1831, doi:10.5194/acp-3-1817-2003, 2003. 23079
Dulac, F., Arboledas, L. A., Alastuey, A., Ancellet, G., Arndt, J., Attié, J.-L., Augustin, P., Becagli, S., Bergametti, G., Bocquet, M., Bordier, F., Bourdon, A., Bourrianne, T., Bravo-Aranda, J., Carrer, D., Ceamanos, X., Chazette, P., Chiapello, I., Comeron, A., D'Amico, G., D'Anna, B., Delbarre, H., Denjean, C., Desboeufs, K., Descloitres, J., Diouri, M., Biagio, C. D., Iorio, T. D., Sarra, G. D., Doppler, L., Durand, P., Amraoui, L. E., Ellul, R., Ferré, H., Fleury, L., Formenti, P., Freney, E., Gaimoz, C., Gerasopoulos, E., Goloub, P., Gomez-Amo, J., Granados-Munoz, M., Grand, N., Grobner, J., Rascado, J.-L. G., Guieu, C., Hadjimitsis, D., Hamonou, E., Hansson, H., Iarlori, M., Ioannou, S., Jambert, C., Jaumouillé, E., Jeannot, M., Junkermann, W., Keleshis, C., Kokkalis, P., Lambert, D., Laurent, B., Léon, J.-F., Liousse, C., Bartolome, M. L., Losno, R., Mallet, M., Mamouri, R.-E., Meloni, D., Menut, L., Montoux, N., Baquero, R. M., Nabat, P., Navas-Guzman, F., Nicolae, D., Nicolas, J., Notton, G., Ohayon, W., Paoli, C., Papayannis, A., Pelon, J., Pey, J., Pont, V., Pujadas, M., Querol, X., Ravetta, F., Renard, J.-B., Rizi, V., Roberts, G., Roujean, J.-L., Sartelet, K., Savelli, J.-L., Sciare, J., Sellegri, K., Sferlazzo, D., Sicard, M., Smyth, A., Solmon, F., Tanré, D., Torres, B., Totems, J., Sanchez, A. T., Verdier, N., Vignelles, D., Vincent, J., Wagner, F., Wang, Y., Wenger, J., and Yassaa, N.: Overview of the Project ChArMEx activities on Saharan Dust in the Mediterranean region, in: 7th Int.

ACPD
14, 23075–23123, 2014

Workshop on Sand/Duststorms and Associated Dustfall, 2–4 December 2013, Frascati, Italy, http://dustworkshop2013.enea.it/presentations/index.php (last access: 2 September 2014), 2013. 23080
EEA: Air quality in Europe, 2013 EEA report, 9, Copenhagen, Denmark, 2013. 23077
Grell, G. A. and Devenyi, D.: A generalized approach to parameterizing convection combining ensemble and data assimilation techniques, Geophys. Res. Lett., 29, 1693, doi:10.1029/2002GL015311, 2002. 23085
Guenther, A., Karl, T., Harley, P., Wiedinmyer, C., Palmer, P. I., and Geron, C.: Estimates of global terrestrial isoprene emissions using MEGAN (Model of Emissions of Gases and Aerosols from Nature), Atmos. Chem. Phys., 6, 3181–3210, doi:10.5194/acp-6-3181-2006, 2006. 23086
Hong, S. Y., Dudhia, J., and Chen, S.: A revised approach to ice microphysical processes for the bulk parameterization of clouds and precipitation, Mon. Weather Rev., 132, 103–120, 2004. 23085
Hong, S. Y., Noh, Y., and Dudhia, J.: A new vertical diffusion package with an explicit treatment of entrainment processes, Mon. Weather Rev., 134, 2318–2341, doi:10.1175/MWR3199.1, 2006. 23085
Honoré, C., Rouïl, L., Vautard, R., Beekmann, M., Bessagnet, B., Dufour, A., Elichegaray, C., Flaud, J., Malherbe, L., Meleux, F., Menut, L., Martin, D., Peuch, A., Peuch, V., and Poisson, N.: Predictability of European air quality: the assessment of three years of operational forecasts and analyses by the PREV'AIR system, J. Geophys. Res., 113, D04301, doi:10.1029/2007JD008761, 2008. 23088
Hsu, N., Tsay, S., King, M., and Herman, J.: Aerosol properties over bright-reflecting source regions, IEEE T. Geosci. Remote, 42, 557–569, 2004. 23084
Israelevich, P., Ganor, E., Alpert, P., Kishcha, P., and Stupp, A.: Predominant transport paths of Saharan dust over the Mediterranean Sea to Europe, J. Geophys. Res., 117, D02205, doi:10.1029/2011JD016482, 2012. 23078
Jiménez-Guerrero, P., Jorba, O., Pay, M. T., Montávez, J. P., Jerez, S., Gómez-Navarro, J. J., and Baldasano, J. M.: Comparison of two different sea-salt aerosol schemes as implemented in air quality models applied to the Mediterranean Basin, Atmos. Chem. Phys., 11, 4833–4850, doi:10.5194/acp-11-4833-2011, 2011. 23079

ACPD
14, 23075–23123, 2014

Kallos, G., Kotroni, V., Lagouvardos, K., and Papadopoulos, A.: On the long-range transport of air pollutants from Europe to Africa, Geophys. Res. Lett., 25, 619–622 doi:10.1029/97GL03319, 1998. 23078

Kallos, G., Papadopoulos, A., Katsafados, P., and Nickovic, S.: Transatlantic Saharan dust transport: model simulation and results, J. Geophys. Res., 111, D09204, doi:10.1029/2005JD006207, 2006. 23079

Kaufman, Y., Tanré, D., Remer, L., Vermote, E., Chi, A., and Holben, B.: Operational remote sensing of tropospheic aerosol over land from EOS moderate resolution imaging spectroradiometer, J. Geophys. Res., 102, 17051–17067, 1997. 23084

Kloog, I., Coull, B., Zanobetti, A., Koutrakis, P., and Schwartz, J.: Acute and chronic effects of particles on hospital admissions in New-England, PLoS One, 7, e34664, doi:10.1371/journal.pone.0034664, 2012. 23077

Kubilay, N., Cokacar, T., and Oguz, T.: Optical properties of mineral dust outbreaks over the northeastern Mediterranean, J. Geophys. Res., 108, D214666, doi:10.1029/2003JD003798, 2003. 23078, 23079

Kulmala, M., Asmi, A., Lappalainen, H. K., Baltensperger, U., Brenguier, J.-L., Facchini, M. C., Hansson, H.-C., Hov, Ø., O'Dowd, C. D., Pöschl, U., Wiedensohler, A., Boers, R., Boucher, O., de Leeuw, G., Denier van der Gon, H. A. C., Feichter, J., Krejci, R., Laj, P., Lihavainen, H., Lohmann, U., McFiggans, G., Mentel, T., Pilinis, C., Riipinen, I., Schulz, M., Stohl, A., Swietlicki, E., Vignati, E., Alves, C., Amann, M., Ammann, M., Arabas, S., Artaxo, P., Baars, H., Beddows, D. C. S., Bergström, R., Beukes, J. P., Bilde, M., Burkhart, J. F., Canonaco, F., Clegg, S. L., Coe, H., Crumeyrolle, S., D'Anna, B., Decesari, S., Gilardoni, S., Fischer, M., Fjaeraa, A. M., Fountoukis, C., George, C., Gomes, L., Halloran, P., Hamburger, T., Harrison, R. M., Herrmann, H., Hoffmann, T., Hoose, C., Hu, M., Hyvärinen, A., Hõrrak, U., Iinuma, Y., Iversen, T., Josipovic, M., Kanakidou, M., Kiendler-Scharr, A., Kirkevåg, A., Kiss, G., Klimont, Z., Kolmonen, P., Komppula, M., Kristjánsson, J.-E., Laakso, L., Laaksonen, A., Labonnote, L., Lanz, V. A., Lehtinen, K. E. J., Rizzo, L. V., Makkonen, R., Manninen, H. E., McMeeking, G., Merikanto, J., Minikin, A., Mirme, S., Morgan, W. T., Nemitz, E., O'Donnell, D., Panwar, T. S., Pawlowska, H., Petzold, A., Pienaar, J. J., Pio, C., Plass-Duelmer, C., Prévôt, A. S. H., Pryor, S., Reddington, C. L., Roberts, G., Rosenfeld, D., Schwarz, J., Seland, Ø., Sellegri, K., Shen, X. J., Shiraiwa, M., Siebert, H., Sierau, B., Simpson, D., Sun, J. Y., Topping, D., Tunved, P., Vaattovaara, P., Vakkari, V., Veefkind, J. P., Visschedijk, A., Vuollekoski, H., Vuolo, R., Wehner, B., Wildt, J., Wood-

ACPD
14, 23075–23123, 2014

ward, S., Worsnop, D. R., van Zadelhoff, G.-J., Zardini, A. A., Zhang, K., van Zyl, P. G., Kerminen, V.-M., S Carslaw, K., and Pandis, S. N.: General overview: European Integrated project on Aerosol Cloud Climate and Air Quality interactions (EUCAARI) – integrating aerosol research from nano to global scales, Atmos. Chem. Phys., 11, 13061–13143, doi:10.5194/acp-11-13061-2011, 2011. 23079

Lelieveld, J., Berresheim, H., Borrmann, S., Crutzen, P. J., Dentener, F. J., Fischer, H., Feichter, J., Flatau, P. J., Heland, J., Holzinger, R., Korrmann, R., Lawrence, M. G., Levin, Z., Markowicz, K. M., Mihalopoulos, N., Minikin, A., Ramanathan, V., Reus, M. D., Roelofs, G. J., Scheeren, H. A., Sciare, J., Schlager, H., Schultz, M., Siegmund, P., Steil, B., Stephanou, E. G., Stier, P., Traub, M., Warneke, C., Williams, J., and Ziereis, H.: Global air pollution crossroads over the Mediterranean, Science, 298, 794–799, 2002. 23079

Levy, R. C., Remer, L. A., Kleidman, R. G., Mattoo, S., Ichoku, C., Kahn, R., and Eck, T. F.: Global evaluation of the Collection 5 MODIS dark-target aerosol products over land, Atmos. Chem. Phys., 10, 10399–10420, doi:10.5194/acp-10-10399-2010, 2010. 23084

Mallet, M.: Overview of the ChArMEx-Aerosol Direct Radiative Forcing on the Mediterranean Climate (ADRIMED) project, in: AMA conference, 20–22 January 2014, Toulouse, 2014. 23080, 23082

Mallet, M., Pont, V., Liousse, C., Roger, J., and Dubuisson, P.: Simulation of aerosol radiative properties with the ORISAM-RAD model during a pollution event (ESCOMPTE 2001), Atmos. Environ., 40, 7696–7705, doi:10.1016/j.atmosenv.2006.08.031, 2006. 23079

Mallet, M., Dubovik, O., Nabat, P., Dulac, F., Kahn, R., Sciare, J., Paronis, D., and Léon, J. F.: Absorption properties of Mediterranean aerosols obtained from multi-year ground-based remote sensing observations, Atmos. Chem. Phys., 13, 9195–9210, doi:10.5194/acp-13-9195-2013, 2013. 23079

Martinelli, N., Olivieri, O., and Girelli, D.: Air particulate matter and cardiovascular disease: a narrative review, Eur. J. Intern. Med., 24, 295–302, doi:10.1016/j.ejim.2013.04.001, 2013. 23077

Menut, L. and Bessagnet, B.: Atmospheric composition forecasting in Europe, Ann. Geophys., 28, 61–74, doi:10.5194/angeo-28-61-2010, 2010. 23079

Menut, L., Goussebaile, A., Bessagnet, B., Khvorostiyanov, D., and Ung, A.: Impact of realistic hourly emissions profiles on modelled air pollutants concentrations, Atmos. Environ., 49, 233–244, 2012. 23086

ACPD
14, 23075–23123, 2014

Menut, L., Bessagnet, B., Khvorostyanov, D., Beekmann, M., Blond, N., Colette, A., Coll, I., Curci, G., Foret, G., Hodzic, A., Mailler, S., Meleux, F., Monge, J.-L., Pison, I., Siour, G., Turquety, S., Valari, M., Vautard, R., and Vivanco, M. G.: CHIMERE 2013: a model for regional atmospheric composition modelling, Geosci. Model Dev., 6, 981–1028, doi:10.5194/gmd-6-981-2013, 2013a. 23080, 23085, 23093

Menut, L., Perez Garcia-Pando, C., Haustein, K., Bessagnet, B., Prigent, C., and Alfaro, S.: Relative impact of roughness and soil texture on mineral dust emission fluxes modeling, J. Geophys. Res., 118, 6505–6520, doi:10.1002/jgrd.50313, 2013b. 23079, 23086

Millan, M., Salvador, R., Mantilla, E., and Kallos, G.: Photo-oxidant dynamics in the Western Mediterranean in Summer: results from European research projects, J. Geophys. Res., 102, D7, 8811–8823, 1997. 23078

Millan, M., Estrela, M. J., Sanz, M. J., Mantilla, E., Martan, M., Pastor, F., Salvador, R., Vallejo, R., Alonso, L., Gangoiti, G., Ilardia, J., Navazo, M., Albizuri, A., Artano, B., Ciccioli, P., Kallos, G., Carvalho, R. A., Andreas, D., Hoff, A., Werhahn, J., and Seufert, G., and Versino, B.: Climatic feedbacks and desertification: the Mediterranean model, J. Climate, 18, 684–701, 2005. 23078

Mlawer, E., Taubman, S., Brown, P., Iacono, M., and Clough, S.: Radiative transfer for inhomogeneous atmospheres: RRTM a validated correlated-k model for the longwave, J. Geophys. Res., 102, 16663–16682, 1997. 23085

Monks, P., Granier, C., Fuzzi, S., Stohl, A., Williams, M., Akimoto, H., Amann, M., Baklanov, A., Baltensperger, U., Bey, I., Blake, N., Blake, R., Carslaw, K., Cooper, O., Dentener, F., Fowler, D., Fragkou, E., Frost, G., Generoso, S., Ginoux, P., Grewe, V., Guenther, A., Hansson, H., Henne, S., Hjorth, J., Hofzumahaus, A., Huntrieser, H., Isaksen, I., Jenkin, M., Kaiser, J., Kanakidou, M., Klimont, Z., Kulmala, M., Laj, P., Lawrence, M., Lee, J., Liousse, C., Maione, M., McFiggans, G., Metzger, A., Mieville, A., Moussiopoulos, N., Orlando, J., O'Dowd, C., Palmer, P., Parrish, D., Petzold, A., Platt, U., Pöschl, U., Prévôt, A., Reeves, C., Reimann, S., Rudich, Y., Sellegri, K., Steinbrecher, R., Simpson, D., ten Brink, H., Theloke, J., van der Werf, G., Vautard, R., Vestreng, V., Vlachokostas, C., and von Glasow, R.: Atmospheric composition change – global and regional air quality, Atmos. Environ., 43, 5268–5350, doi:10.1016/j.atmosenv.2009.08.021, 2009. 23078

Nabat, P., Solmon, F., Mallet, M., Kok, J. F., and Somot, S.: Dust emission size distribution impact on aerosol budget and radiative forcing over the Mediterranean region: a regional cli-

ACPD
14, 23075–23123, 2014

mate model approach, Atmos. Chem. Phys., 12, 10545–10567, doi:10.5194/acp-12-10545-2012, 2012. 23079

Pérez, C., Haustein, K., Janjic, Z., Jorba, O., Huneeus, N., Baldasano, J. M., Black, T., Basart, S., Nickovic, S., Miller, R. L., Perlwitz, J. P., Schulz, M., and Thomson, M.: Atmospheric dust modeling from meso to global scales with the online NMMB/BSC-Dust model – Part 1: Model description, annual simulations and evaluation, Atmos. Chem. Phys., 11, 13001–13027, doi:10.5194/acp-11-13001-2011, 2011. 23079

Putaud, J.-P., Van Dingenen, R., Dell'Acqua, A., Raes, F., Matta, E., Decesari, S., Facchini, M. C., and Fuzzi, S.: Size-segregated aerosol mass closure and chemical composition in Monte Cimone (I) during MINATROC, Atmos. Chem. Phys., 4, 889–902, doi:10.5194/acp-4-889-2004, 2004. 23094

Querol, X., Pey, J., Pandolfi, M., Alastuey, A., Cusack, M., Pereza, N., Moreno, T., Viana, M., Mihalopoulos, N., Kallo, G., and Kleanthous, S.: African dust contributions to mean ambient PM10 mass-levels across the Mediterranean Basin, Atmos. Environ., 43, 4266–4277, 2009. 23079

Rodriguez, S., Querol, X., Alastuey, A., and de la Rosa, J.: Atmospheric particulate matter and air quality in the Mediterranean: a review, Environ. Chem. Lett., 5, 1–7, doi:10.1007/s10311-006-0071-0, 2007. 23078

Sayer, A. M., Hsu, N. C., Bettenhausen, C., and Jeong, M.-J.: Validation and uncertainty estimates for MODIS Collection 6 "Deep Blue" aerosol data, J. Geophys. Res.Atmos., 118, 7864–7872, doi:10.1002/jgrd.50600, 2013. 23090

Scheeren, H. A., Lelieveld, J., Roelofs, G. J., Williams, J., Fischer, H., de Reus, M., de Gouw, J. A., Warneke, C., Holzinger, R., Schlager, H., Klüpfel, T., Bolder, M., van der Veen, C., and Lawrence, M.: The impact of monsoon outflow from India and Southeast Asia in the upper troposphere over the eastern Mediterranean, Atmos. Chem. Phys., 3, 1589–1608, doi:10.5194/acp-3-1589-2003, 2003. 23078

Skamarock, W., Klemp, J., Dudhia, J., Gill, D., Barker, D., Wang, W., and Powers, J.: A description of the advanced research WRF version 2, NCAR/TN-468+STR, NCAR Technical Note, Boulder, Colorado, USA, 2007. 23084

Tanré, D., Kaufman, Y., Herman, M., and Mattoo, S.: Remote sensing of aerosol properties over oceans using the MODIS/EOS sprectral radiances, J. Geophys. Res., 102, 16971–16988, doi:10.1029/96JD03437, 1997. 23084

ACPD
14, 23075–23123, 2014

Turquety, S., Menut, L., Bessagnet, B., Anav, A., Viovy, N., Maignan, F., and Wooster, M.: API-FLAME v1.0: high-resolution fire emission model and application to the Euro-Mediterranean region, Geosci. Model Dev., 7, 587–612, doi:10.5194/gmd-7-587-2014, 2014. 23079, 23081, 23084, 23086

Von Storch, H., Langenberg, H., and Feser, F.: A spectral nudging technique for dynamical downscaling purposes, Mon. Weather Rev., 128, 3664–3673, 2000. 23085

Wild, O., Zhu, X., and Prather, M. J.: Fast-J: Accurate simulation of in- and below-cloud photolysis in tropospheric chemical models, J. Atmos. Chem., 37, 245–282, 2000. 23086

ACPD
14, 23075–23123, 2014

Table 1. Characteristics of the AirBase and AERONET (Aerosol RObotic NETwork) stations used in this study. Note that the AirBase Italian stations of Chitignano, Baceno, Schivenoglia and Vercelli provide daily averaged values, when all other stations provide hourly (but not regular) measurements.

Site	Country	Longitude	Latitude
ADRIMED measurements sites			
Lampedusa	Italy	12.63	35.51
Cape Corsica	France	9.41	42.83
AirBase coastal "background" stations			
Zorita	Spain	−0.16	40.73
Cartagena	Spain	−0.97	37.60
Malaga	Spain	−4.46	36.72
Ajaccio	France	8.73	41.92
Bastia	France	9.44	42.69
Hyeres	France	6.13	43.11
Taranto	Italy	17.28	40.41
Chitignano	Italy	11.90	43.66
AirBase continental "background" stations			
Aranjuez	Spain	−3.59	40.04
LaCiguena	Spain	−2.42	42.46
Cordoba	Spain	−4.77	37.90
Agen	France	0.62	44.19
Champforgeuil	France	4.83	46.82
Gap	France	6.07	44.55
Baceno	Italy	8.25	46.31
Schivenoglia	Italy	11.07	44.99
Vercelli	Italy	8.40	45.31
AERONET stations			
Banizoumbou	Nigeria	2.66	13.54
Capo Verde	Capo Verde	−22.93	16.73
Dakar	Senegal	−16.95	14.39
Cinzana	Mali	−5.93	13.28
Ilorin	Nigeria	4.340	8.32
Izana	Canaries, Spain	−16.49	28.31
Forth Crete	Greece	25.27	35.31
Lampedusa	Italy	12.63	35.51
Saada	Morocco	−8.15	31.61
Zinder Airport	Nigeria	8.98	13.75

ACPD
14, 23075–23123, 2014

Table 2. List of ATR flights for the tropospheric measurements of meteorological variables, ozone (O_3) and carbon monoxyde (CO) concentrations (ppb). N_{data} corresponds to the number of data after averaging the high temporal frequency of aircraft measurements to a constant 5 mn time step.

Flight no.	Date	J_{day}	Decimal hour	N_{data}
28	14 Jun 2013	165	9.05	46
29	16 Jun 2013	167	7.55	36
30	16 Jun 2013	167	11.49	40
31	17 Jun 2013	168	6.76	39
32	17 Jun 2013	168	11.18	32
33	19 Jun 2013	170	11.04	49
34	20 Jun 2013	171	9.83	54
35	22 Jun 2013	173	7.57	47
36	22 Jun 2013	173	12.75	40

ACPD
14, 23075–23123, 2014

Table 3. Correlations (R), Root Mean Squared Error (RMSE) and bias of measured and modelled daily maximum value of surface O_3 concentrations ($\mu g\,m^{-3}$), for representative AirBase stations.

Site	N_{obs}	O_3 daily max ($\mu g\,m^{-3}$) Obs	Mod	R	RMSE
AirBase coastal "background" stations					
Zorita	37	110.65	105.17	0.66	14.87
Cartagena	41	102.37	113.49	0.42	16.80
Malaga	40	113.60	101.50	0.09	24.15
Ajaccio	38	107.21	101.09	0.41	17.72
Bastia	41	114.80	97.27	0.21	25.02
Hyeres	41	118.59	95.70	0.55	29.33
Taranto	41	116.83	123.81	0.71	12.91
Chitignano	40	99.38	113.66	0.17	26.13
AirBase continental "background" stations					
Aranjuez	38	113.26	113.78	0.33	21.35
LaCiguena	41	102.34	97.46	0.55	21.63
Cordoba	41	127.32	113.63	0.57	20.82
Agen	41	95.32	95.83	0.71	19.26
Champforgeuil	38	99.26	99.85	0.53	21.51
Gap	39	98.36	103.95	0.32	16.79
Baceno	39	117.03	104.62	0.29	21.47
Vercelli	39	124.41	131.74	0.15	34.69

ACPD
14, 23075–23123, 2014

Table 4. Correlations (R), Root Mean Squared Error (RMSE) and bias of measured and modelled of hourly surface O_3 concentrations ($\mu g\,m^{-3}$), for representative AirBase stations.

Site	N_{obs}	O_3 hourly ($\mu g\,m^{-3}$) Obs	Mod	R	RMSE
AirBase coastal "background" stations					
Zorita	815	74.00	84.93	0.62	30.45
Cartagena	956	73.40	93.72	0.49	31.08
Malaga	907	87.18	87.79	0.28	25.26
Ajaccio	892	72.96	79.92	0.45	25.15
Bastia	978	90.82	76.05	0.30	27.80
Hyeres	983	86.49	67.72	0.57	31.10
Taranto	575	90.15	98.12	0.69	20.25
Chitignano	892	72.39	88.83	0.51	28.14
AirBase continental "background" stations					
Aranjuez	841	79.69	83.14	0.63	22.84
LaCiguena	978	72.30	78.95	0.54	25.31
Cordoba	945	90.95	89.43	0.74	19.41
Agen	977	64.59	74.89	0.61	26.05
Champforgeuil	836	61.86	76.23	0.57	33.59
Gap	917	66.08	90.93	0.21	36.75
Baceno	913	86.26	91.30	0.51	21.35
Vercelli	898	85.06	93.69	0.66	27.87

ACPD
14, 23075–23123, 2014

Table 5. Correlations (R), Root Mean Squared Error (RMSE) and bias of measured and modelled daily mean Aerosol Optical Depth, for several AERONET stations.

Site	N_{obs}	$\overline{AOD}$ daily mean (ad.) Obs	Mod	R	RMSE
Banizoumbou	357	0.59	0.46	0.27	0.47
Capo Verde	166	0.49	0.47	0.57	0.16
Dakar	248	0.53	0.65	0.52	0.21
Cinzana	338	0.58	0.45	0.52	0.34
Ilorin	104	0.38	0.44	0.12	0.52
Izana	516	0.05	0.15	0.76	0.14
Lampedusa	238	0.16	0.22	0.85	0.08
Saada	410	0.24	0.26	0.65	0.15
Zinder Airport	345	0.56	0.68	0.26	0.57
Forth Crete	108	0.11	0.17	0.36	0.09

ACPD
14, 23075–23123, 2014

Table 6. Correlation (R), bias and RMSE for the daily mean PM_{10} ($\mu g\,m^{-3}$) surface concentrations (except for the Lampedusa measurements corresponding to Total Suspended Particles).

Site	N_{obs}	PM_{10} daily mean ($\mu g\,m^{-3}$)		R	RMSE
		Obs	Mod		
ADRIMED measurements sites					
Lampedusa	700	36.76	33.78	0.20	18.07
Cape Corsica	527	11.62	27.67	0.09	19.11
AirBase coastal "background" stations					
Zorita	816	16.25	16.13	0.58	8.99
Cartagena	955	21.62	24.26	−0.02	12.73
Malaga	905	32.53	31.17	−0.08	19.85
Ajaccio	733	20.93	27.21	0.12	11.07
Bastia	887	21.10	25.20	0.10	9.15
Hyeres	955	29.26	26.36	0.69	6.27
Taranto	935	19.79	21.45	0.48	7.05
AirBase continental "background" stations					
Chitignano	72	10.35	19.80	0.57	9.66
Aranjuez	843	23.24	15.18	0.42	12.78
LaCiguena	976	23.19	14.81	0.46	10.05
Cordoba	941	21.56	23.94	0.23	18.38
Agen	983	14.47	16.61	−0.04	9.69
Champforgeuil	972	15.89	17.51	0.16	9.78
Gap	822	12.93	13.69	0.57	4.99
Baceno	33	7.88	12.26	0.37	9.06
Schivenoglia	73	26.93	20.88	0.20	13.77
Vercelli	40	16.08	19.40	0.62	7.21

ACPD
14, 23075–23123, 2014

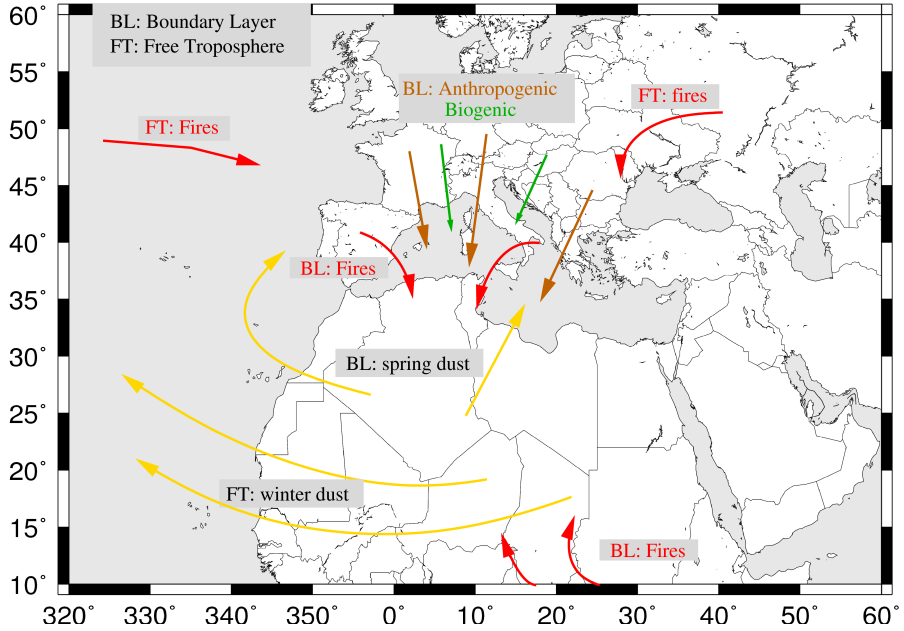

Figure 1. Synthesis of all aerosols types crossing the Mediterranean area.

ACPD
14, 23075–23123, 2014

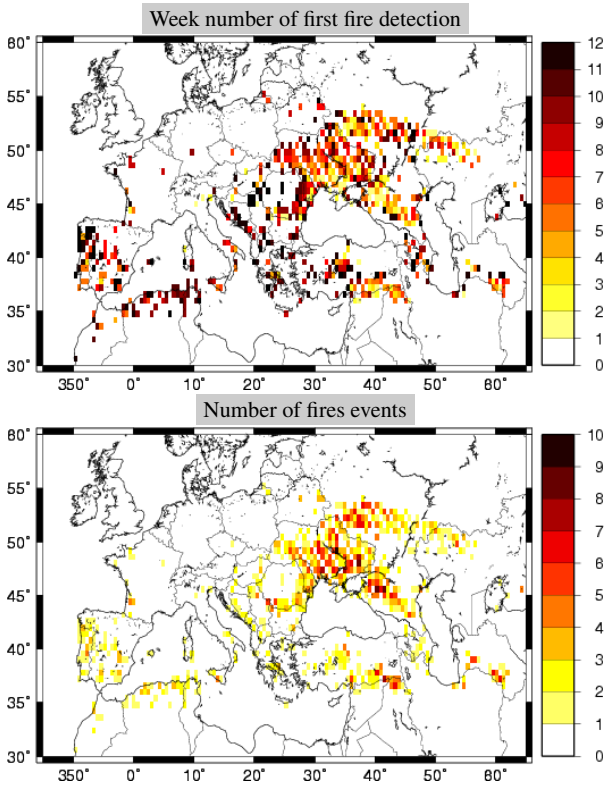

Figure 2. Synthesis of vegetation fires events observed during the summer of 2013, from the 1 June to the 31 August. (Top) Week of first detection, (bottom) number of events.

ACPD
14, 23075–23123, 2014

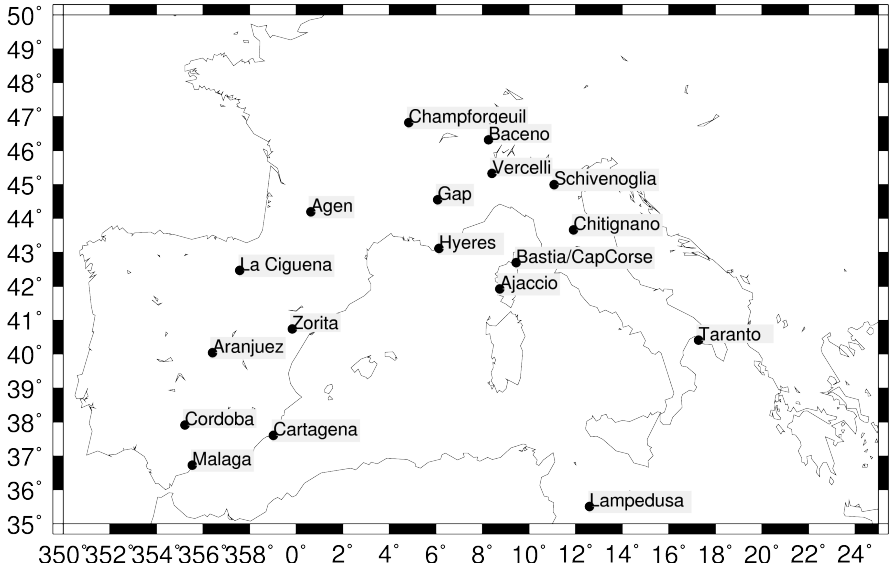

Figure 3. Locations of the AirBase stations providing O_3 and PM_{10} measurements used in this study.

ACPD
14, 23075–23123, 2014

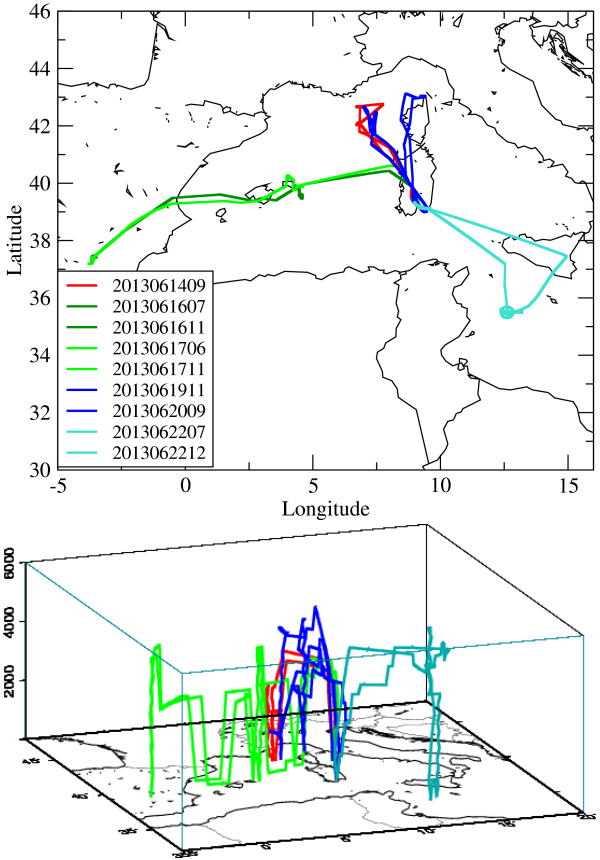

Figure 4. ATR-42 trajectories for the flight of the 14 June (red), 16 and 17 June (blue), 19 and 20 June (green) and 22 June (green-blue).

ACPD
14, 23075–23123, 2014

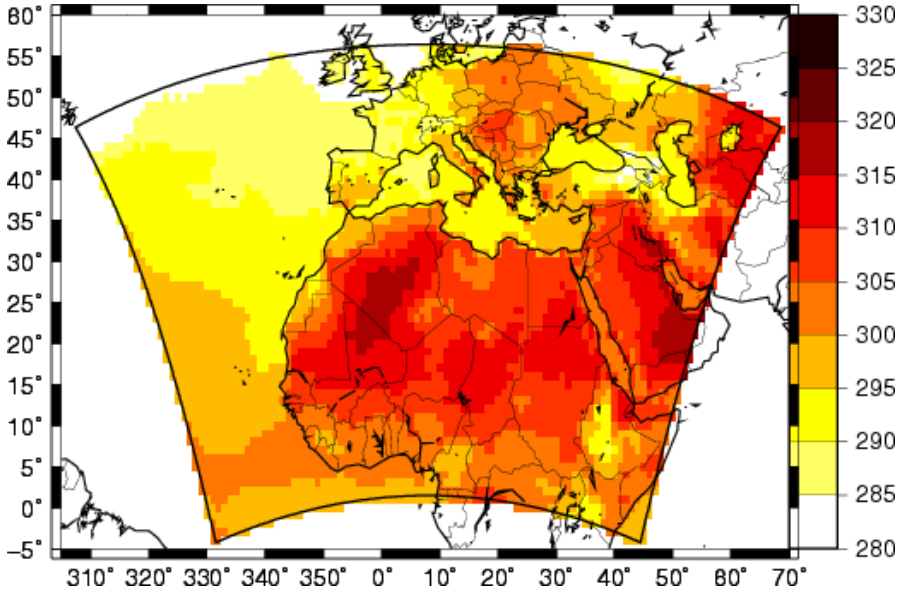

Figure 5. The simulation domain for WRF and CHIMERE. A Lambert conformal projection is used with a constant horizontal resolution of 50 km × 50 km. Colors represent the 2 m temperature (in Kelvin) for the 21 June 12:00 UTC, and the vectors represent the 10 m wind speed.

ACPD
14, 23075–23123, 2014

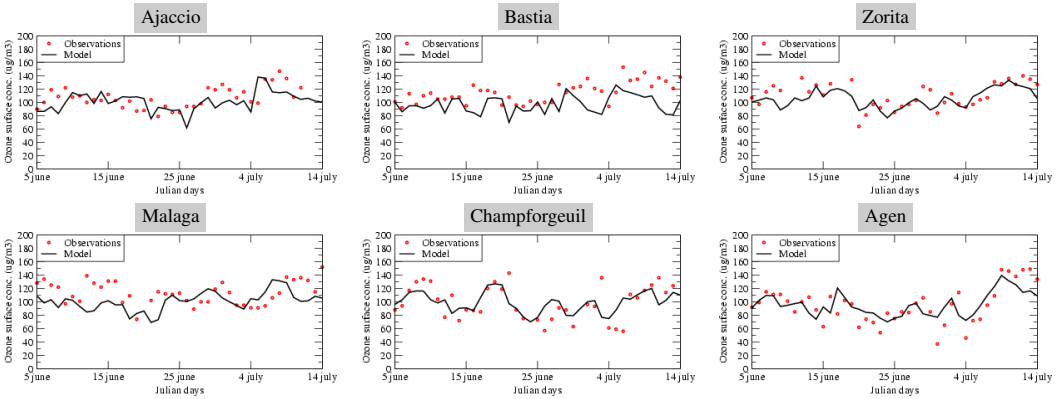

Figure 6. Time series of daily maximum of O_3 surface concentrations for some selected AirBase sites, continental and coastal stations.

ACPD
14, 23075–23123, 2014

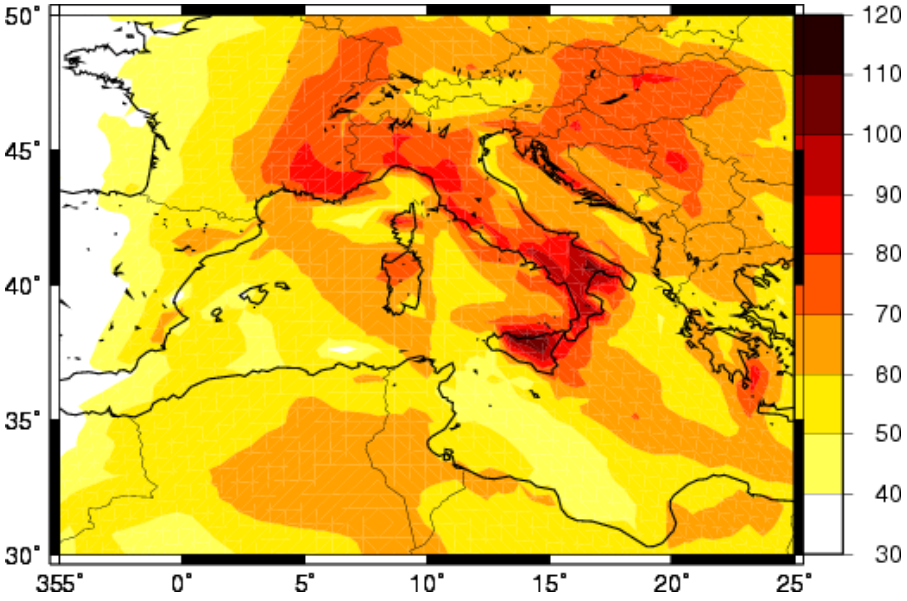

Figure 7. Surface ozone concentrations (ppb) map for the 17 June 2013, 12:00 UTC.

ACPD
14, 23075–23123, 2014

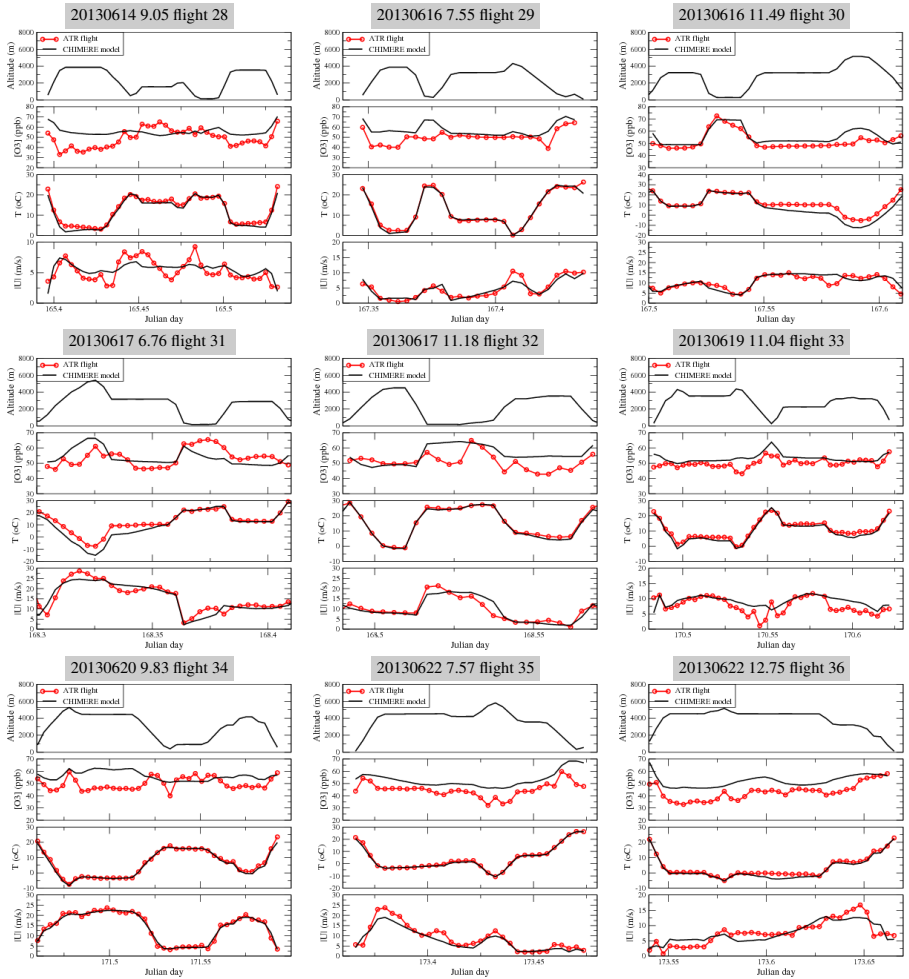

Figure 8. O_3 concentrations, temperature and wind speed along the flight trajectories.

ACPD
14, 23075–23123, 2014

Analysis of the atmospheric composition during the summer 2013

L. Menut et al.

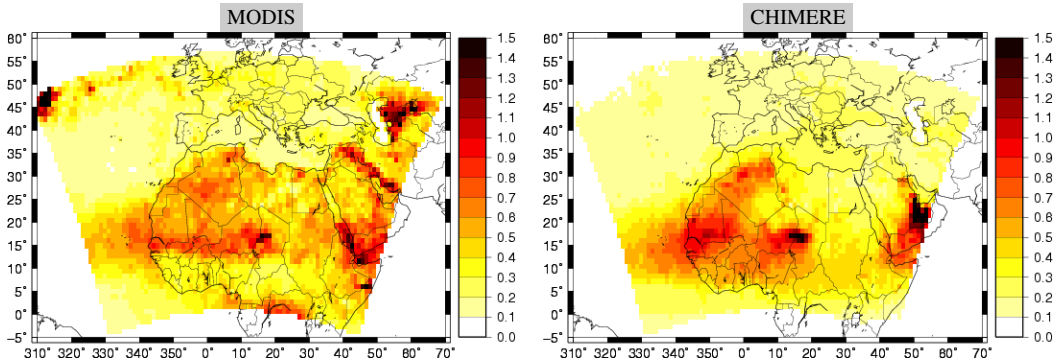

Figure 9. Comparison of Aerosol Optical Depth measured by MODIS (left) and modelled with CHIMERE (right). This AOD corresponds to the mean averaged value over the period from 6 June to 15 July 2013.

ACPD
14, 23075–23123, 2014

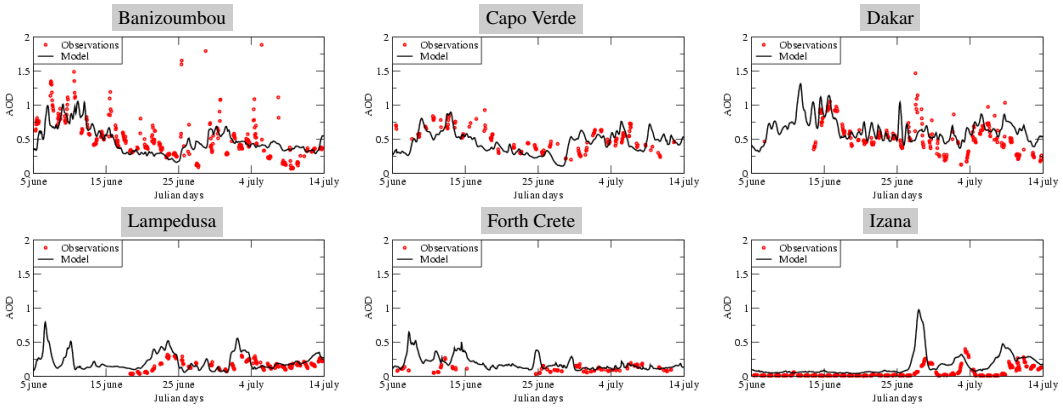

Figure 10. Time series of hourly Aerosol Optical Depth (AOD) for selected AERONET stations.

ACPD
14, 23075–23123, 2014

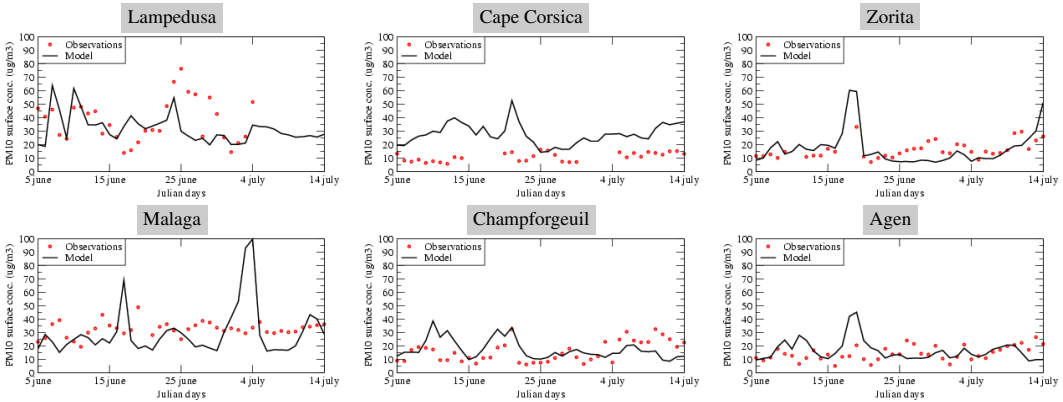

Figure 11. Time series of daily averaged PM_{10} surface concentrations for the ADRIMED sites (Lampedusa and Cape Corsica) and some selected AirBase sites, continental and coastal stations (except for the Lampedusa measurements corresponding to Total Suspended Particles).

ACPD
14, 23075–23123, 2014

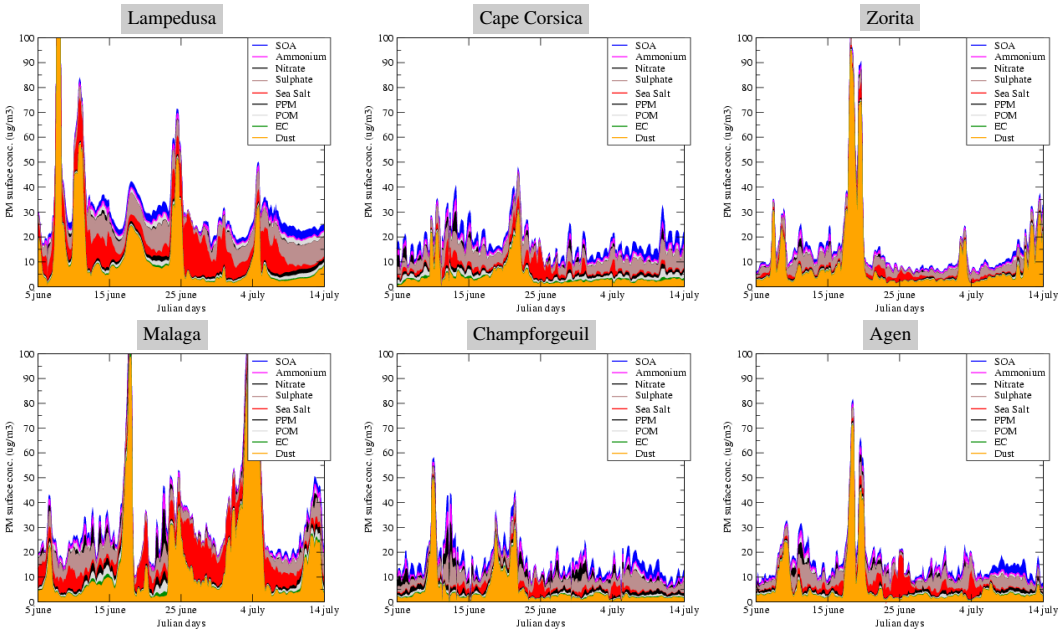

Figure 12. Time series of hourly surface concentrations of all modelled aerosols for the ADRIMED sites (Lampedusa and Cape Corsica) and some selected AirBase sites, continental and coastal stations.

ACPD
14, 23075–23123, 2014

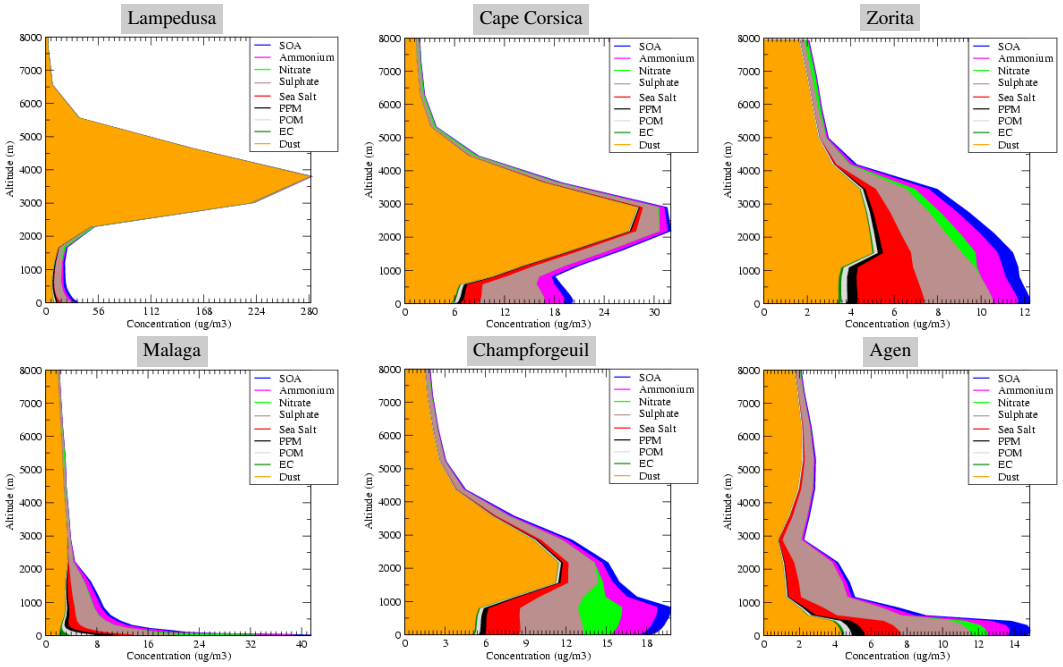

Figure 13. Vertical profiles of all modelled aerosols for the 21 June 2013. Results are presented for the ADRIMED sites (Lampedusa and Cape Corsica) and some selected AirBase sites, continental and coastal stations.

ACPD
14, 23075–23123, 2014

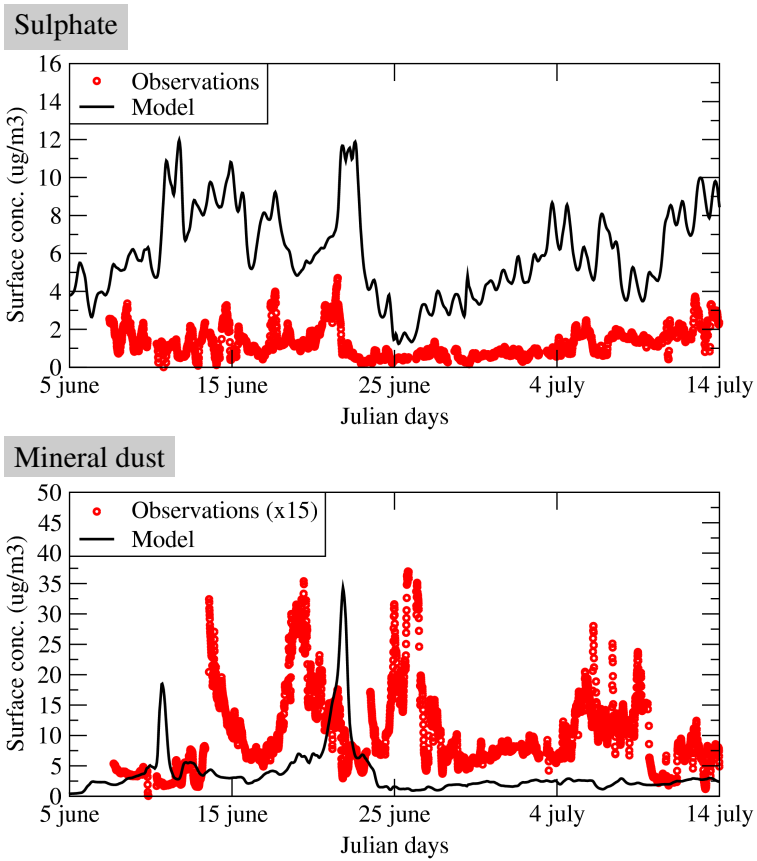

Figure 14. Surface concentrations comparisons between measurements for Sulphate and Dust at Cape Corsica site and corresponding modelled values. The measured Calcium is multiplied by 15 to be comparable to modelled mineral dust.

ACPD
14, 23075–23123, 2014